Journal of Bone and Mineral Metabolism (2019) 37:967–975
https://doi.org/10.1007/s00774-019-01014-y

ORIGINAL ARTICLE

The *Shisa3* knockout mouse exhibits normal bone phenotype

Kohei Murakami[1] · He Zhifeng[2] · Takako Suzuki[3] · Yasuhiro Kobayashi[2] · Yukio Nakamura[3]

Received: 18 February 2019 / Accepted: 28 May 2019 / Published online: 20 June 2019

Abstract
Wnt signaling is important for both skeletal development and bone disease, with Wnt inhibitory factors playing critical roles in bone metabolism. SHISA3 blocks the maturation and transportation of Frizzled receptors to the cell surface, thereby inhibiting the Wnt/*β*-catenin signaling pathway in lung cancer. However, the function of Shisa3 in bone biology remains uninvestigated. This study found that Shisa3 was strongly expressed in the calvarial bones of mice, especially in osteoblasts. In addition, adenovirus-mediated gene transfer of murine Shisa3 significantly inhibited Wnt3a-induced nuclear translocation of *β*-catenin and mRNA expression of the Wnt target gene *Axin2*. In bone phenotype assessments of *Shisa3* knockout (*Shisa3* KO) mice, micro-computed tomography, mRNA expressions of osteoblast markers, and skeletal preparations all displayed no significant differences compared with *Shisa3* wild-type mice. mRNA expression analysis of canonical Wnt signaling target genes (*Axin2*, *Lef1*, *Dkk1*, and *Tnfrsf11b*) in calvarial bones at P0.5 also revealed no significant findings. In $Axin2^{Cre/ERT2}$ knock-in mice, the number of *Axin2*-expressing cells in the calvariae of *Shisa3* KO and control mice were comparable. Thus, there appears to be a redundancy in the function of Shisa3 in bone development, likely with other Shisa family members.

Keywords Shisa3 · Osteoblast · Wnt inhibitor · Bone formation

Introduction

Wnt signaling has important roles in both skeletal development and bone disease. Several genes involved in Wnt signaling contribute to congenital skeletal abnormalities and the development of bone metabolic diseases. Hypofunctional alleles of *WNT1* cause autosomal-recessive osteogenesis imperfecta [1], and abnormal *WNT4*, *WNT5B*, and *WNT16* genes influence bone mineral density [2–4]. Wnt inhibitory factors also play critical roles in bone metabolism. For example, osteocytes secrete the *SOST* gene product sclerostin that binds to lipoprotein receptor-related protein (LRP) 5/6 and inhibits canonical Wnt signaling [5], and loss-of-function mutations in *SOST* markedly increase bone mass [6, 7]. A single allele of the *DKK1*, which inhibits Wnt signaling by binding to LRP6 [8, 9], leads to increases in bone mass as well [10].

Shisa family members were first identified as proteins involved in head formation in *Xenopus* [11]. Shisa blocks the maturation and transportation of Frizzled receptors to the cell surface, thereby inhibiting the Wnt/*β*-catenin signaling pathway to regulate developmental processes [11]. Eight Shisa members (Shisa2−Shisa9) have been described to date in vertebrates. In the only study exploring the function of human SHISA3, the protein suppressed metastasis and tumorigenesis in lung cancers through interactions with all known Frizzled receptors in the endoplasmic reticulum [12]. However, the role of SHISA3 in bone biology remains largely unknown.

This study examined the function of murine Shisa3 in bone metabolism. Shisa3 was strongly expressed in osteoblast lineage cells in calvariae and inhibited canonical Wnt signaling. However, a Shisa3 deficiency neither affected Wnt signaling in bone tissues nor altered osteogenesis.

Electronic supplementary material The online version of this article (https://doi.org/10.1007/s00774-019-01014-y) contains supplementary material, which is available to authorized users.

✉ Yukio Nakamura
yxn14@shinshu-u.ac.jp

[1] Department of Oral and Maxillofacial Radiology, School of Dentistry, Matsumoto Dental University, 1780 Gobara, Hirooka, Shiojiri 399-0781, Japan

[2] Institute for Oral Science, Matsumoto Dental University, Shiojiri, Nagano, Japan

[3] Department of Orthopaedic Surgery, Shinshu University School of Medicine, 3-1-1 Asahi, Matsumoto, Nagano 390-8621, Japan

Our findings indicate a redundancy in the function of Shisa3 in murine osteoblasts.

Materials and methods

Mice

mShisa3 mutant mice created at the RIKEN Center for Developmental Biology [13] were kindly provided. The mice were generated by replacing a 437-bp sequence spanning from 176 bp upstream of the translation initiation site to a part of the succeeding intron with the *LacZ-neo* cassette, with the deleted exon encoding the signal peptide and first cysteine-rich domain. Both *Axin2*$^{Cre/ERT2}$ mice (Stock#018867) and *Rosa26*^{tdTomato} mice (Stock#007914) were purchased from Jackson Laboratories. Animal experiments were performed in compliance with the 3Rs, and all efforts were made to minimize suffering. All procedures for animal care were approved by the Animal Management Committee of Matsumoto Dental University (permit number 326) and performed accordingly.

Cell cultures

Primary murine calvarial cells were isolated from the calvariae of neonates, as previously described [14]. Twenty calvariae were collected and subjected to sequential digestions using PBS containing 0.1% collagenase and 0.2% dispase. Cells isolated in fractions 2, 3, and 4 were combined and cultured in α-MEM containing 10% FBS on two dishes (10 cm in diameter) until high confluency. The cells were then detached from the dishes by typsin-EDTA, suspended on 12 dishes (10 cm in diameter) for 4 days, and stored at − 80 °C. These primary osteoblasts were cultured in 6-well plates or cover glasses for 2 days and subjected to experiments.

Bone marrow macrophages (BMMs) and mature osteoclasts were obtained, as previously described [15]. First, mice were killed by cervical dislocation, and bone marrow cells were collected by flushing the tibiae. The bone marrow cells were cultured in α-MEM containing 10% FBS in the presence of Csf1 (50 ng ml^{-1}) on dishes (60 mm in diameter). Non-adherent cells containing osteoclast precursors were harvested and seeded onto 48-well plates in the presence of Csf1 for 2 days, and adherent cells were further cultured with Csf1 in the presence or absence of GST-RANKL (200 ng ml^{-1}; Oriental Yeast) for 3 days. The cells without GST-RANKL were collected as BMM. Mature osteoclasts induced by RANKL were confirmed as tartrate-resistant acid phosphatase-positive multinuclear cells and collected.

Quantitative reverse transcription-PCR (qPCR) analysis

qPCR was performed as described elsewhere [16]. Primer sets were purchased from Takara Bio Inc. mRNA levels were calculated by normalization to the house keeping gene *hypoxanthine phosphoribosyl transferase* (*Hprt1*) using the $\Delta\Delta C_T$ method.

Immunofluorescence histochemistry

To examine Shisa3 localization, calvariae from *Shisa3-LacZ* knock-in mice at P7 were subjected to immunofluorescence analysis. Frozen sections of 20 μm thickness were cut using a cryostat and stained with anti-β-galactosidase antibody (Z378B; Promega, 1:100) with a Vector M.O.M. immunodetection kit by the protocol specified by the manufacturer (Vector Laboratories). Stained slides were mounted with Vectashield (Vector Laboratories) and analyzed using a confocal laser scanning system (LSM 510; CarlZeiss).

Adenovirus-mediated gene transfer

Adenoviruses expressing *LacZ* or *Shisa3* were prepared as follows: a plasmid vector with a murine Shisa3 (mShisa3) sequence was obtained from OriGene (MR216748), and PCR fragments containing the mShisa3 sequence were ligated into a pAdenoX-CMV-ZsGreen vector (Takara Clontech). For controls, fragments containing a LacZ sequence were cloned into the vector. The linearized vectors were transfected into human embryonic kidney 293T cells to produce adenoviruses according to the manufacturer's instructions. Primary osteoblasts were cultured with each adenovirus for 24 h before the addition of recombinant Wnt3a (R&D Systems, 50 ng ml^{-1}). Eight hours later, we fixed the cells for immunocytochemistry or isolated total RNA for qPCR analysis.

Immunoblotting analysis

Immunoblotting was performed as previously described [15] using the following antibodies: anti-SHISA3 rabbit pAb (SAB3500826; Sigma, 1:1000), anti-β-galactosidase antibody (Z378B; Promega, 1:1000), anti-α tubulin mouse mAb (CP06; Calbiochem, 1:1000), donkey anti-rabbit IgG-HRP (NA934V; GE Healthcare, 1:5000), and goat anti-mouse IgG-HRP (170-6516; Bio-Rad Laboratories, 1:10000).

Immunocytochemistry

Immunocytochemistry was carried out as previously described [16] using the following antibodies: anti-β-catenin rabbit mAb (ab32572; abcam, 1:250) and donkey anti-rabbit IgG NL557-conjugated pAb (NL004; R&D Systems, 1:200).

Micro-computed tomography (micro-CT) analysis

Micro-CT analysis (ScanXmate-A080, Comscan Tecno) was performed on P0.5, 8-week-old, and 24-week-old mice to examine for morphological changes and assess morphological indices. Calvaria thickness was determined in bone tissues located between 0.5 and 5.5 mm from the maxillary third molars using image analysis software (TRI/3D-BON, Ratoc System Engineering). Indices of the distal metaphysis in femurs were calculated in trabecular bones located between 0.5 and 1.5 mm from the growth plates.

Skeletal preparations

New-born mice were eviscerated, fixed in 95% ethanol overnight, and transferred into acetone. One day later, they were stained with Alcian blue (0.03% [*w/v*], 80% ethanol, and 20% acetic acid) overnight. The samples were then destained by initially washing in two changes of 70% ethanol and incubated in 95% ethanol overnight. Thereafter, they were treated with 1% potassium hydroxide for 1 h and stained with Alizarin red S (0.005% [*w/v*] and 1% potassium hydroxide) for 3 h. The specimens were kept in 50% glycerol-0.5% potassium hydroxide at 4 °C until the skeletons became clearly visible. For storage, the specimens were transferred into 50%, 80%, and finally, 100% glycerol.

Induction of Cre-mediated recombination

Tamoxifen (T-5648; Sigma) was dissolved in corn oil by sonication for 15 min at 37 °C, and 2 mg of tamoxifen/30 g of body weight was intraperitoneally injected into *Axin2*$^{Cre/ERT}$; *Rosa26*^{tdTomato}; *Shisa3*$^{+/-}$ mice and *Axin2*$^{Cre/ERT2}$; *Rosa26*^{tdTomato}; *Shisa3*$^{-/-}$ mice at P7. The mice were allowed to recover for 3 days and then killed.

Statistical analyses

All cell culture experiments were performed in triplicate and similar results were obtained. Statistical analysis was performed using Prism7 software (GraphPad). Results were analyzed using Welch's *t* test or 1-way ANOVA. When 1-way ANOVA showed statistical significance, the data were

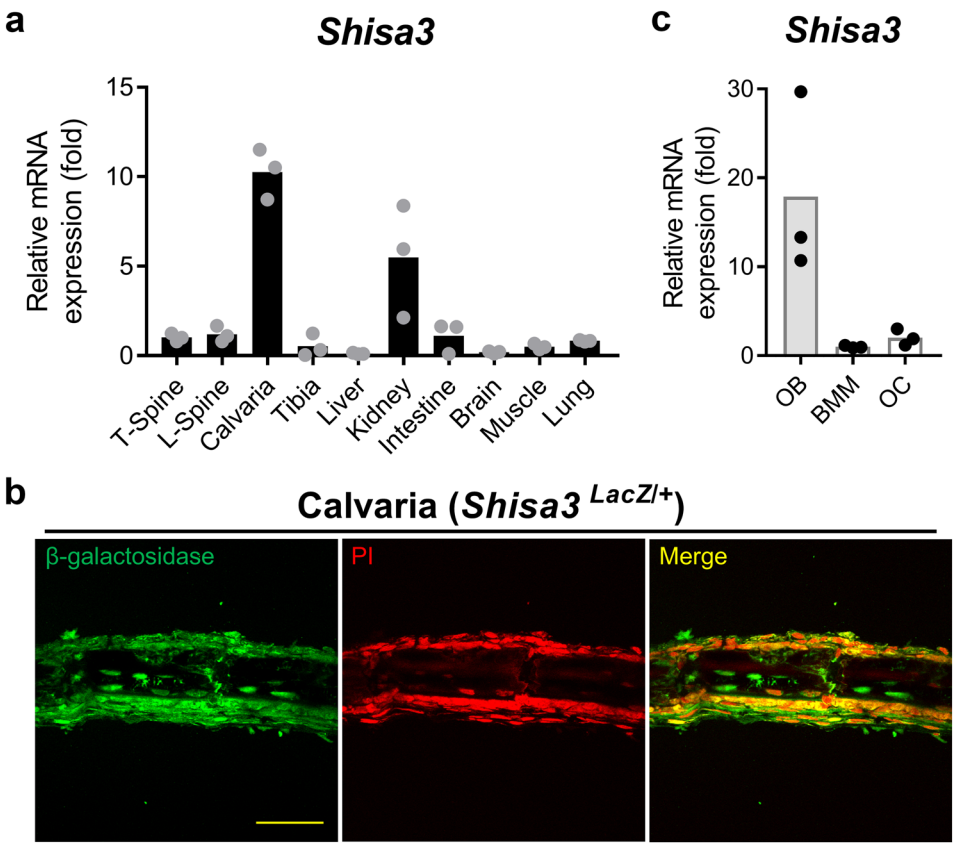

Fig. 1 Expression of *Shisa3* in mice. **a** Tissue distribution of *Shisa3* mRNA in new-born mice. T-Spine, thoracic spine; L-Spine, lumbar spine. **b** β-galactosidase expression in calvarial bone derived from a new-born *Shisa3* $^{LacZ/+}$ mouse. Cell nuclei were stained with PI (red). Scale bar, 50 µm. **c** *Shisa3* mRNA expression in osteoblasts (OB), bone marrow macrophages (BMM), and osteoclasts (OC). Profiling of the OB (*Runx2*), BMM (*Rank*), and OC (*Ctsk*) marker gene expressions were previously shown [16] (color figure online)

compared using the Tukey–Kramer test. A P value of less than 0.05 was considered statistically significant.

Results

Expression of *Shisa3* in mice

qPCR analysis was performed on various tissues obtained from new-born mice to examine *Shisa3* expression. The highest levels of *Shisa3* were found in the calvaria (Fig. 1a), with low expression in other bone tissues (Fig. 1a). We confirmed that calvarial bone cells strongly expressed *Shisa3* using *Shisa3-LacZ* knock-in mice at P7 (Fig. 1b). Then, the *Shisa3* transcripts were primarily osteoblasts rather than bone marrow macrophages or mature osteoclasts (Fig. 1c).

Murine Shisa3 inhibits Wnt signaling

Since human SHISA3 is known as an inhibitor of Wnt signaling, we investigated the function of murine Shisa3 using adenovirus-mediated gene transfer. After treatment with the same multiplicity of infection (MOI) of adenovirus, primary osteoblasts derived from calvaria were cultured for an additional day. Successful infection of the control (Ad-*LacZ*) or *Shisa3*-expressing (Ad-*Shisa3*) adenovirus was detected as ZsGreen-positive cells (Fig. 2a), and protein expression was confirmed by immunoblotting (Fig. 2b). Recombinant Wnt3a induced the nuclear translocation of β-catenin in primary osteoblasts (Fig. 2c), whereas the adenovirus-mediated gene transfer of *Shisa3* impaired it (Fig. 2c). Wnt3a also evoked an increase in a target gene of Wnt signaling, *Axin2*, in osteoblasts (Fig. 2d). The forced expression of murine *Shisa3* significantly attenuated Wnt3a-induced *Axin2* expression (Fig. 2d), suggesting that Shisa3 could inhibit canonical Wnt signaling.

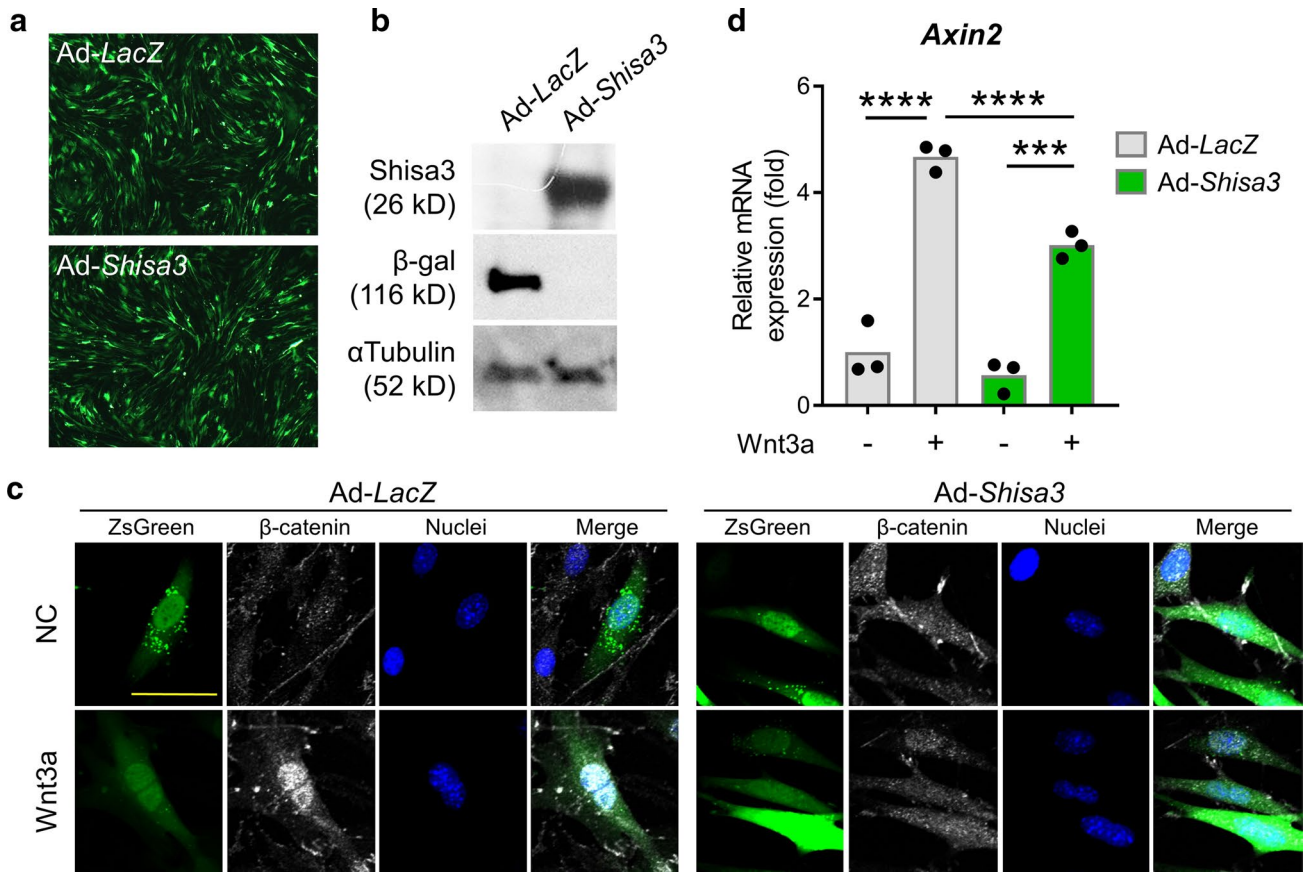

Fig. 2 Overexpression of murine Shisa3 abrogates canonical Wnt signaling. **a** Adenovirus infection detected as ZsGreen-positive osteoblasts. **b** Immunoblot images of β-galactosidase (β-gal) or Shisa3 expression. Uncropped images of the blots are shown in Supplementary Fig. S1. **c**, **d** Effects of Ad-*Shisa3* on Wnt3a-induced (50 ng ml^{-1}) nuclear translocation of β-catenin or expression of the canonical Wnt target gene *Axin2* in osteoblasts. Cell nuclei were stained with TO-PRO®-3 (blue). Scale bar, 50 µm. ***$P < 0.001$, ****$P < 0.0001$, Tukey–Kramer test (color figure online)

Shisa3 deficiency does not affect skeletal development

The in vitro findings prompted us to examine the roles of Shisa3 in the development of calvarial bone using Shisa3 knockout (*Shisa3*$^{-/-}$) mice. The mice were generated by replacing the first coding exon and a part of the succeeding intron with the *LacZ*-neo cassette; therefore, homozygous knock-in mice were null for Shisa3. *Shisa3* was confirmed to be deleted in *Shisa3*$^{-/-}$ mice (Fig. 3a). Then, comparisons of P0.5 *Shisa3*$^{-/-}$ mice and littermates were made by micro-CT analysis of heads. No remarkable phenotypes were detected in the knockout mice (Fig. 3b). Similarly, no significant difference was observed in head examinations of 8-week-old male *Shisa3*$^{-/-}$ mice, and calvarial bone thickness was comparable to that of littermates (Fig. 3c, d). Comparable results were seen in 24-week-old male mice (Supplementary Fig. S2). Calvarial bone tissues from P0.5 mice were examined for the mRNA expressions of osteoblast-specific transcriptional factors (*Runx2* and *Sp7*) and differentiation marker genes (*Col1a1* and *Bglap*). There were no significant differences among *Shisa3*$^{+/+}$, *Shisa3*$^{+/-}$, and

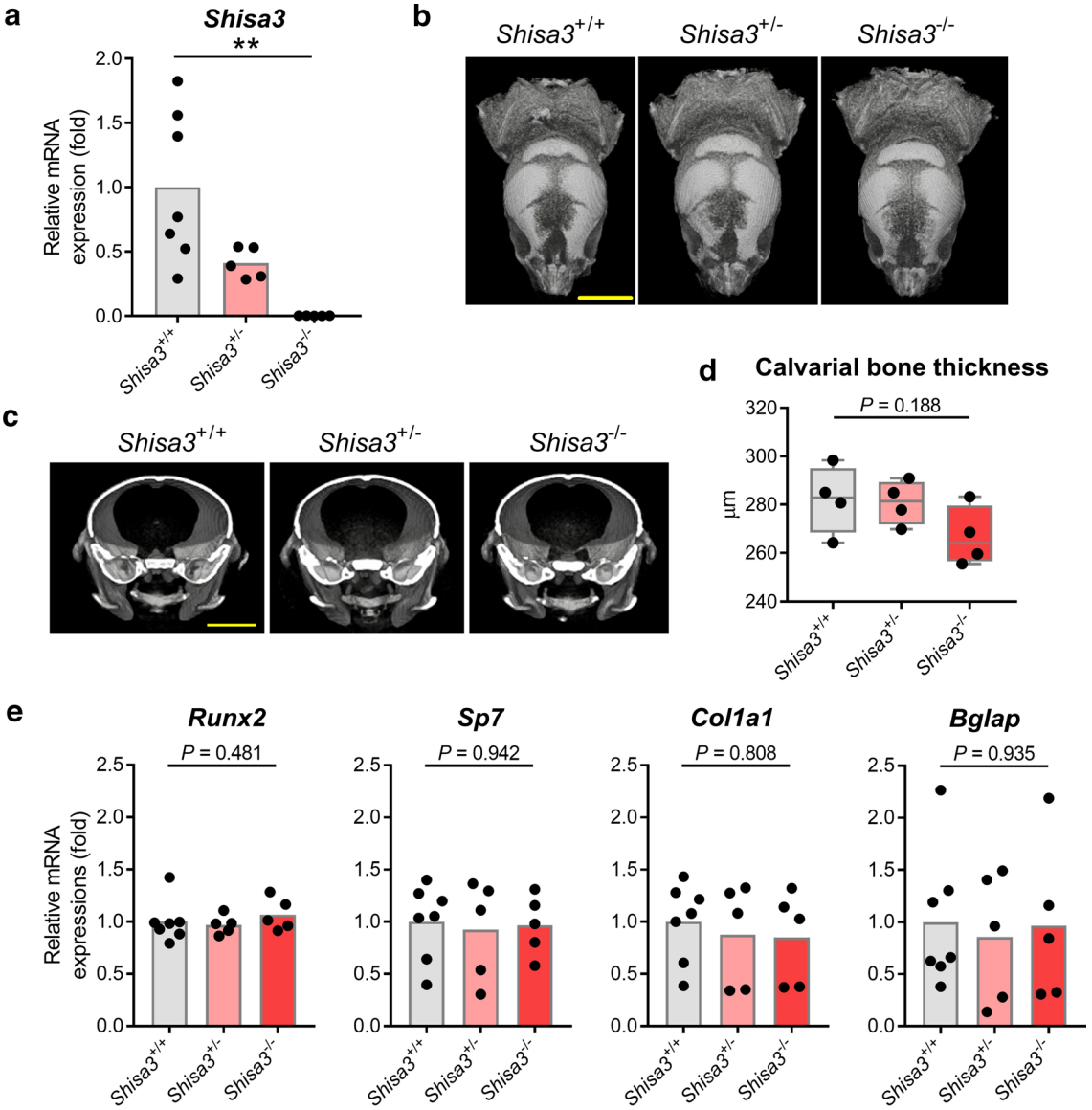

Fig. 3 Shisa3 KO mice exhibit normal calvarial bone formation. **a** *Shisa3* mRNA expression levels in calvarial bones at P0.5. $^{**}P < 0.01$, Tukey–Kramer test. **b**, **c** Representative micro-CT images of the heads of *Shisa3*$^{+/+}$, *Shisa3*$^{+/-}$, and *Shisa3*$^{-/-}$ mice at P0.5 (**b**) and 8 weeks old (**c**). Scale bar, 3.5 mm. $n = 4$ for each genotype. **d** Calvarial bone thickness of 8-week-old mice determined by micro-CT analysis. *P* value was calculated by ANOVA. **e** Osteoblast marker gene expressions in calvarial bones. *P* values were calculated by ANOVA. *Sp7* Sp7 transcription factor 7 (Osterix), *Col1a1* Collagen, type I, alpha 1, *Bglap* Bone gamma carboxyglutamate protein

Shisa3$^{-/-}$ mice (Fig. 3e). Skeletal preparations also revealed no remarkable phenotypes in skeletal tissues, including the head (Fig. 4). Micro-CT of distal femurs from 8-week-old male and female *Shisa3*$^{-/-}$ mice showed no significant differences in bone volume, number of trabeculae, trabecular thickness, or trabecular separation (Supplementary Fig. S3). We next analyzed calvariae from *Shisa3*$^{+/+}$, *Shisa3*$^{+/-}$, and *Shisa3*$^{-/-}$ mice at P0.5 to determine the mRNA expressions of canonical Wnt signaling target genes (*Axin2*, *Lef1*, *Dkk1*, and *Tnfrsf11b*); however, no significant differences were seen among the groups (Fig. 5a). We also assessed the expression of the Wnt target *Axin2* using an *Axin2*$^{Cre/ERT2}$ knock-in allele crossed to the *Cre* reporter *Rosa26*^{tdTomato}. *Axin2*$^{Cre/ERT2}$; *Rosa26*^{tdTomato}; *Shisa3*$^{+/-}$ and *Axin2*$^{Cre/ERT2}$; *Rosa26*^{tdTomato}; *Shisa3*$^{-/-}$ mice were administered tamoxifen at P7 and analyzed at P10. Confocal images revealed that the number of Tomato-positive cells in the calvariae of *Shisa3*$^{-/-}$ mice did not change significantly compared with that in *Shisa3*$^{+/-}$ mice (Fig. 5b, c). Collectively, these findings indicated that a Shisa3 deficiency affected neither canonical Wnt signaling nor osteoblast differentiation in vivo.

Discussion

This study revealed that *Shisa3* was strongly expressed in murine calvarial bone, especially in osteoblasts. Since Shisa3 overexpression inhibited canonical Wnt signaling in vitro, we expected the protein to play a role in skeletal development. However, a Shisa3 deficiency produced no skeletal abnormality or alteration in canonical Wnt signaling. The absence of phenotypic changes after gene knockout is usually explained by the complementary function of paralogous genes. Accordingly, we determined the mRNA expressions of all Shisa family members in the calvaria. qPCR analysis clarified that murine calvariae expressed *Shisa2*, *Shisa4*, and *Shisa5* in addition to *Shisa3* (Supplementary Fig. S4a). Calvariae from Shisa3-deficient mice also expressed *Shisa2*, *Shisa4*, and *Shisa5* (Supplementary

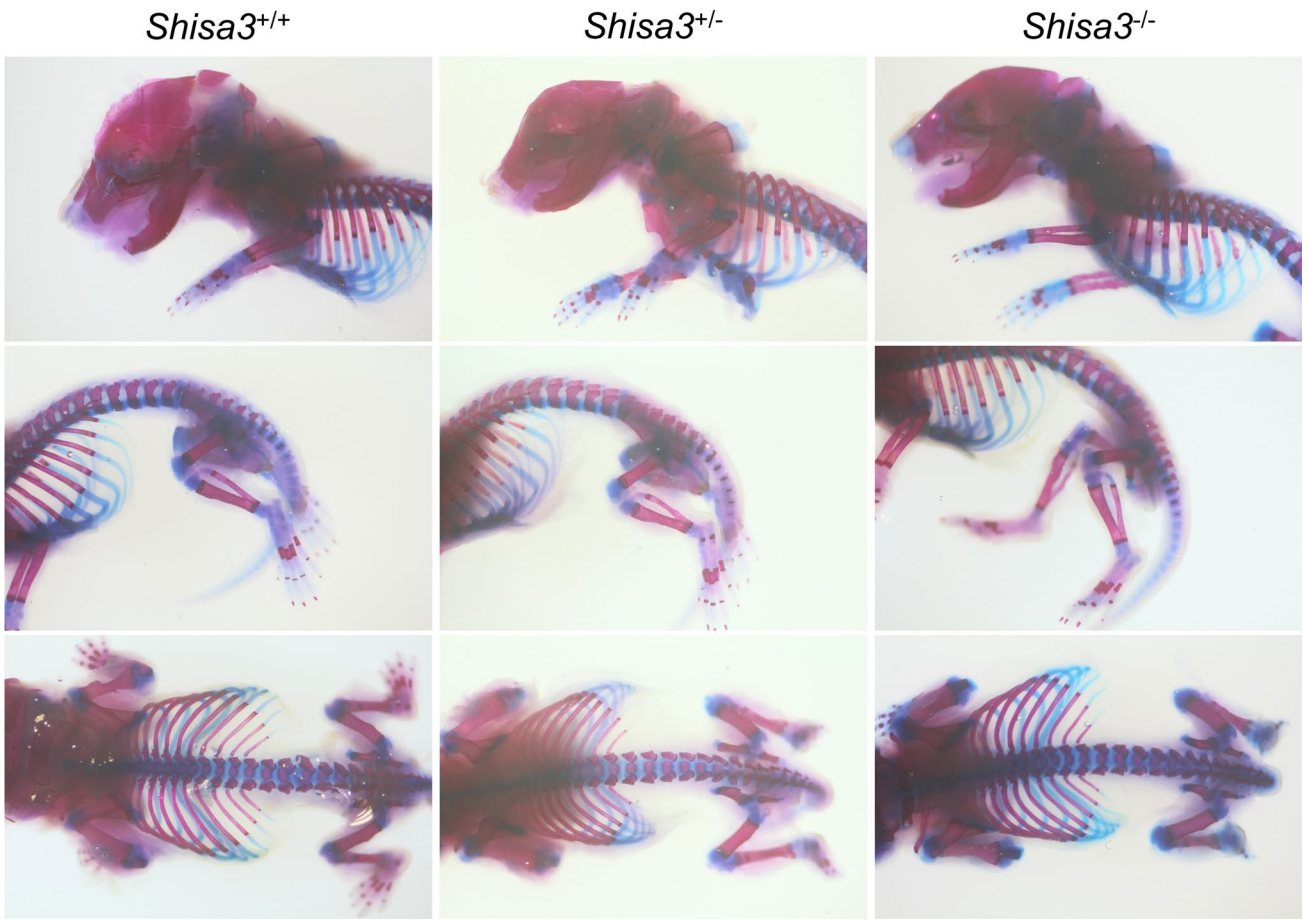

Fig. 4 Shisa3 KO mice exhibit normal skeletal development. Skeletons of wild-type, heterozygous, and homozygous genotype mice at P0.5. $n = 3$ for each genotype

Fig. S4b). Based on these findings, we speculate a redundancy in the function of Shisa3 in murine osteoblasts.

In this investigation, the expression of *Shisa3* was high in the calvarial bone and particularly in osteoblasts. Interestingly, we found that skeletal tissues derived from the lumbar vertebrae, thoracic vertebrae, and tibia, which also contained osteoblasts, exhibited low levels of *Shisa3* mRNA expressions. Since those skeletal tissues undergo endochondral ossification, Shisa3 may be associated with the process of membranous ossification. A previous study showed that Prx1-cre-induced deletion of *β*-catenin resulted in a loss of calvarial bones [17], indicating that canonical Wnt/*β*-catenin signaling was essential in murine calvarial bones. The reason why expression of the Wnt inhibitor *Shisa3* is high only in the calvaria is unknown at present.

The R-Spondin (RSPO) family was first identified as a secreted activator of Wnt/*β*-catenin signaling in *Xenopus* [18]. RSPO increases the number of cell surface Frizzled receptors by binding to ring finger protein 43 (RNF43) and zinc and ring finger 3 (ZNRF3), which ubiquitinate and degrade Frizzled receptors, thereby amplifying Wnt signaling in a leucine-rich repeat-containing G-protein coupled receptor 4/5/6 (LGR4/5/6) dependent [19–21] or independent [22] manner. Mutations in the *RSPO2* gene lead to limb abnormalities such as tetra-amelia in mice [23–25] and severe limb defects in humans [22]. As the Shisa family also modulates the number of Frizzled receptors on cell membranes, our findings represent an important step in clarifying the relationship between Wnt signals and bone disease.

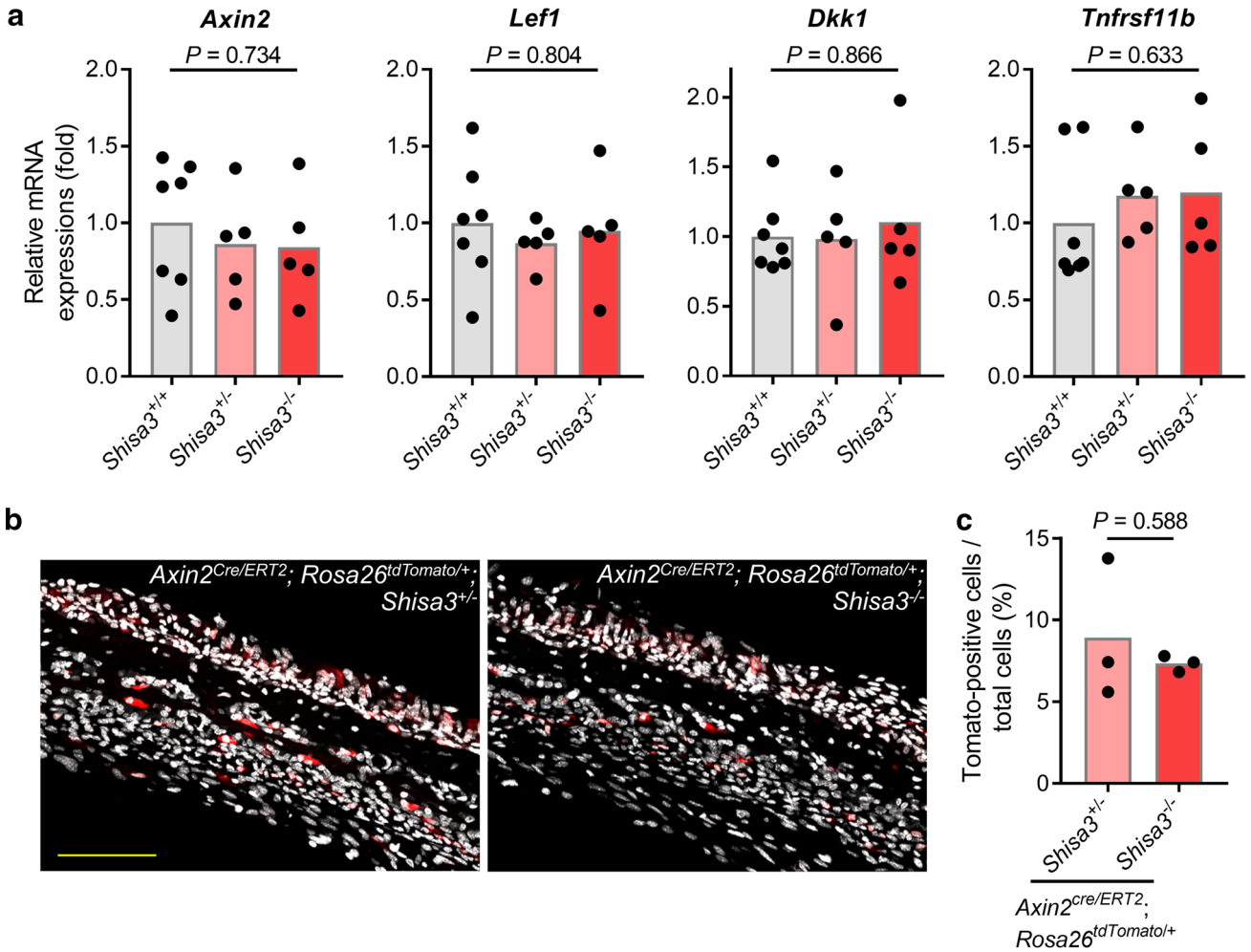

Fig. 5 Presence or absence of Shisa3 does not affect canonical Wnt signaling. **a** Expressions of canonical Wnt target genes in calvarial bones at P0.5. *P* values were calculated by ANOVA. *Lef1* Lymphoid enhancer binding factor 1, *Dkk1* Dickkopf WNT signaling pathway inhibitor 1, *Tnfrsf11b* Tumor necrosis factor receptor superfamily, member 11b (osteoprotegerin). **b** Representative confocal images of calvarial bone sections from P10 $Axin2^{Cre/ERT2/+}$; $Rosa26^{tdTomato/+}$; $Shisa3^{+/-}$ mice and $Axin2^{Cre/ERT2/+}$; $Rosa26^{tdTomato/+}$; $Shisa3^{-/-}$ mice 3 days after tamoxifen injection. Cell nuclei were stained with TO-PRO®-3 (white). Scale bar, 100 µm. **c** Quantification of the frequency of Tomato-positive cells in total cells. $n = 3$. Welch's *t*-test (color figure online)

Although Shisa3 functions as a Wnt inhibitory factor, Shisa3 knockout mice exhibit no remarkable phenotypes in bone tissues, which strengthens the notion of a compensatory mechanism by other members of the Shisa family. The phenotypes of double, triple, and quadruple mutants among *Shisa2*, *Shisa3*, *Shisa4*, and *Shisa5,* therefore, require analysis, although preparation of quadruple mutants remains challenging despite recent advances in gene editing. It was possible that other Wnt antagonists or a yet unidentified protein served a complementary function with Shisa3 [13]. Moreover, we did not examine whether Shisa3 was involved in pathological conditions, such as osteoporosis or tumor bone metastasis. Further study is warranted on the Shisa family regarding the complex interplay between Wnt signaling and bone metabolism and disease.

Acknowledgements The authors would like to thank Yasuhide Furuta at the RIKEN Center for Life Science Technologies for supplying the *Shisa3* knockout mice. The authors deeply thank the members of the bone club at Matsumoto Dental University for their stimulating discussion and warm support.

Compliance with ethical standards

Conflict of interest All the authors declare that they have no conflict of interest.

Inormed concent This study is not an experiment that requires Informed consent.

References

1. Pyott SM, Tran TT, Leistritz DF, Pepin MG, Mendelsohn NJ, Temme RT, Fernandez BA, Elsayed SM, Elsobky E, Verma I, Nair S, Turner EH, Smith JD, Jarvik GP, Byers PH (2013) *WNT1* mutations in families affected by moderately severe and progressive recessive osteogenesis imperfecta. Am J Hum Genet 92:590–597
2. Styrkarsdottir U, Halldorsson BV, Gretarsdottir S, Gudbjartsson DF, Walters GB, Ingvarsson T, Jonsdottir T, Saemundsdottir J, Center JR, Nguyen TV, Bagger Y, Gulcher JR, Eisman JA, Christiansen C, Sigurdsson G, Kong A, Thorsteinsdottir U, Stefansson K (2008) Multiple genetic loci for bone mineral density and fractures. N Engl J Med 358:2355–2365
3. Estrada K, Styrkarsdottir U, Evangelou E, Hsu YH, Duncan EL et al (2012) Genome-wide meta-analysis identifies 56 bone mineral density loci and reveals 14 loci associated with risk of fracture. Nat Genet 44:491–501
4. Zheng HF, Tobias JH, Duncan E, Evans DM, Eriksson J et al (2012) *WNT16* influences bone mineral density, cortical bone thickness, bone strength, and osteoporotic fracture risk. PLoS Genet 8:e1002745
5. Li X, Zhang Y, Kang H, Liu W, Liu P, Zhang J, Harris SE, Wu D (2005) Sclerostin binds to LRP5/6 and antagonizes canonical Wnt signaling. J Biol Chem 280:19883–19887
6. Brunkow ME, Gardner JC, Van Ness J, Paeper BW, Kovacevich BR, Proll S, Skonier JE, Zhao L, Sabo PJ, Fu Y, Alisch RS, Gillett L, Colbert T, Tacconi P, Galas D, Hamersma H, Beighton P, Mulligan J (2001) Bone dysplasia sclerosteosis results from loss of the *SOST* gene product, a novel cystine knot-containing protein. Am J Hum Genet 68:577–589
7. Balemans W, Patel N, Ebeling M, Van Hul E, Wuyts W, Lacza C, Dioszegi M, Dikkers FG, Hildering P, Willems PJ, Verheij JB, Lindpaintner K, Vickery B, Foernzler D, Van Hul W (2002) Identification of a 52 kb deletion downstream of the *SOST* gene in patients with van Buchem disease. J Med Genet 39:91–97
8. Mao B, Wu W, Li Y, Hoppe D, Stannek P, Glinka A, Niehrs C (2001) LDL-receptor-related protein 6 is a receptor for Dickkopf proteins. Nature 411:321–325
9. Bafico A, Liu G, Yaniv A, Gazit A, Aaronson SA (2001) Novel mechanism of Wnt signalling inhibition mediated by Dickkopf-1 interaction with LRP6/Arrow. Nat Cell Biol 3:683–686
10. Morvan F, Boulukos K, Clément-Lacroix P, Roman SR, Suc-Royer I, Vayssière B, Ammann P, Martin P, Pinho S, Pognonec P, Mollat P, Niehrs C, Baron R, Rawadi G (2006) Deletion of a single allele of the *Dkk1* gene leads to an increase in bone formation and bone mass. J Bone Miner Res 21:934–945
11. Yamamoto A, Nagano T, Takehara S, Hibi M, Aizawa S (2005) Shisa promotes head formation through the inhibition of receptor protein maturation for the caudalizing factors, Wnt and FGF. Cell 120:223–235
12. Chen CC, Chen HY, Su KY, Hong QS, Yan BS, Chen CH, Pan SH, Chang YL, Wang CJ, Hung PF, Yuan S, Chang GC, Chen JJ, Yang PC, Yang YC, Yu SL (2014) Shisa3 is associated with prolonged survival through promoting β-catenin degradation in lung cancer. Am J Respir Crit Care Med 190:433–444
13. Furushima K, Yamamoto A, Nagano T, Shibata M, Miyachi H, Abe T, Ohshima N, Kiyonari H, Aizawa S (2007) Mouse homologues of Shisa antagonistic to Wnt and Fgf signalings. Dev Biol 306:480–492
14. Takahashi N, Akatsu T, Udagawa N, Sasaki T, Yamaguchi A, Moseley JM, Martin TJ, Suda T (1988) Osteoblastic cells are involved in osteoclast formation. Endocrinology 123:2600–2602
15. Murakami K, Kobayashi Y, Uehara S, Suzuki T, Koide M, Yamashita T, Nakamura M, Takahashi N, Kato H, Udagawa N, Nakamura Y (2017) A Jak1/2 inhibitor, baricitinib, inhibits osteoclastogenesis by suppressing RANKL expression in osteoblasts in vitro. PLoS One 12:e0181126
16. Murakami K, Kikugawa S, Kobayashi Y, Uehara S, Suzuki T, Kato H, Udagawa N, Nakamura Y (2018) Olfactomedin-like protein OLFML1 inhibits Hippo signaling and mineralization in osteoblasts. Biochem Biophys Res Commun 505:419–425
17. Hill TP, Später D, Taketo MM, Birchmeier W, Hartmann C (2005) Canonical Wnt/β-catenin signaling prevents osteoblasts from differentiating into chondrocytes. Dev Cell 8:727–738
18. Kazanskaya O, Glinka A, del Barco Barrantes I, Stannek P, Niehrs C, Wu W (2004) R-Spondin2 is a secreted activator of Wnt/beta-catenin signaling and is required for Xenopus myogenesis. Dev Cell 7:525–534
19. de Lau W, Barker N, Low TY, Koo BK, Li VS, Teunissen H, Kujala P, Haegebarth A, Peters PJ, van de Wetering M, Stange DE, van Es JE, Guardavaccaro D, Schasfoort RB, Mohri Y, Nishimori K, Mohammed S, Heck AJ, Clevers H (2011) Lgr5 homologues associate with Wnt receptors and mediate R-spondin signalling. Nature 476:293–297
20. Hao HX, Xie Y, Zhang Y, Charlat O, Oster E, Avello M, Lei H, Mickanin C, Liu D, Ruffner H, Mao X, Ma Q, Zamponi R, Bouwmeester T, Finan PM, Kirschner MW, Porter JA, Serluca FC, Cong F (2012) ZNRF3 promotes Wnt receptor turnover in an R-spondin-sensitive manner. Nature 485:195–200
21. Koo BK, Spit M, Jordens I, Low TY, Stange DE, van de Wetering M, van Es JH, Mohammed S, Heck AJ, Maurice MM, Clevers H (2012) Tumour suppressor RNF43 is a stem-cell E3 ligase that induces endocytosis of Wnt receptors. Nature 488:665–669

22. Szenker-Ravi E, Altunoglu U, Leushacke M, Bosso-Lefèvre C, Khatoo M et al (2018) RSPO2 inhibition of RNF43 and ZNRF3 governs limb development independently of LGR4/5/6. Nature 557:564–569
23. Bell SM, Schreiner CM, Wert SE, Mucenski ML, Scott WJ, Whitsett JA (2008) R-spondin 2 is required for normal laryngeal-tracheal, lung and limb morphogenesis. Development 135:1049–1058
24. Nam JS, Park E, Turcotte TJ, Palencia S, Zhan X, Lee J, Yun K, Funk WD, Yoon JK (2007) Mouse R-spondin2 is required for apical ectodermal ridge maintenance in the hindlimb. Dev Biol 311:124–135
25. Aoki M, Kiyonari H, Nakamura H, Okamoto H (2008) R-spondin2 expression in the apical ectodermal ridge is essential for outgrowth and patterning in mouse limb development. Dev Growth Differ 50:85–95